MODELLING AND SIMULATION OF AN INVERTED PENDULUM SYSTEM: COMPARISON BETWEEN EXPERIMENT AND CAD PHYSICAL MODEL

J. S. Sham, M. I. Solihin, F. Heltha and Muzaiyanah H.
Faculty of Engineering, Technology & Built Environment, UCSI University, Kuala Lumpur Campus, Cheras, Kuala Lumpur, Malaysia
E-Mail: jssham@hotmail.com

ABSTRACT

SimMechanics can be used for modelling of mechanical systems of any degree of freedom in MATLAB/Simulink environment. Mechanical systems have physical properties that use physical modelling blocks in SimMechanics that relates to geometric and kinematic. By using this toolbox, it saves the time and effort to derive the equations of motion. SimMechanics provides a visualization and animation of mechanical systems with 3D geometry graphical shown. SimMechanics is able to interact with SolidWorks via external features. This paper describes the development of physical modeling of an inverted pendulum (IP) via SimMechanics. The swing up and stabilizing controller for the IP using Linear Quadratic Regulator (LQR) is also discussed.

Keywords: inverted pendulum, solidworks, simmechanics, MATLAB, lqr controller, swing-up controller.

INTRODUCTION

In many years, there has been a growing interest in IP for wide range of home applications and industrial applications (Olfa Boubaker, 2003). An IP is considered as a good example to cover control engineering applications such as impact force sensor, attitude control of a space booster rocket and a satellite (Olfa Boubaker, 2003). An IP is a combination of nonlinear and open-loop unstable system that makes the control more challenging. Throughout the years, a lot of control tasks are benchmark IP for design, testing, evaluating and comparing to the standard techniques. The IP consists of modular mechanical and electrical hardware which can be easily constructed and suitable for all level of instruction. Figure-1 shows the lab scale rotary IP that can performs swing up and balancing control of IP.

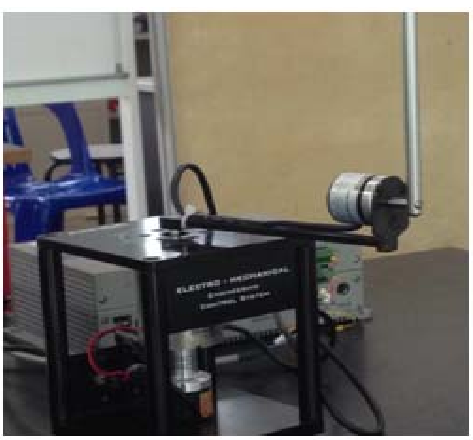

Figure-1. Rotary IP in laboratory.

SimMechanics is implemented since MATLAB software version R2008B or higher. It can interacts with SolidWorks version 2001 or higher. As mentioned above, SimMechanics able to make a multi-body system using blocks whereby each blocks have their own physical properties such as frames and frame transforms (Low, K.H., H. Wang and M.Y. Wang, 2005). Figure-2 shows an IP constructed in SolidWorks. The modelling is built in SolidWorks and exports into SimMechanics via external features.

Figure-2. SolidWorks IP.

LQR Controller is a special case of optimal control that can analytically solved when weighting matrices are selected correctly (Xiumin Diao, Dr. Ou Ma, 2006). The results of the SimMechanics are compared with the result of the real experimental IP.

METHODOLOGY

Block diagrams are automatically created and connected together when import from SolidWorks. Angular position, and angular velocity for arm and pendulum is the main concern throughout the paper. Torque is act as motor input for arm to rotate. Figure-3 shows conversions are made in IP subsystem.

VOL. 10, NO. 20, NOVEMBER 2015 ISSN 1819-6608
ARPN Journal of Engineering and Applied Sciences

www.arpnjournals.com

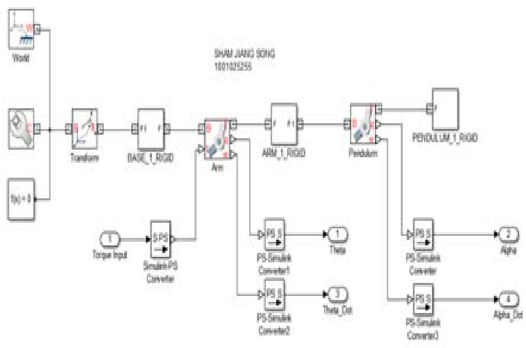

Figure-3. IP subsystem.

Figure-4 shows catch controller subsystem used for the system to automatically detect the angle in between 5° to 25°. A conversion from radian to degree is required to convert output from the IP Subsystem.

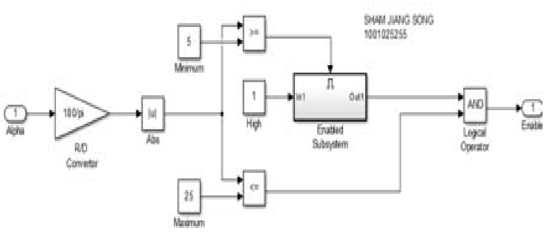

Figure-4. Catch controller subsystem.

Figure-5 shows an enabled subsystem executes HIGH output when HIGH input is received from Enable port.

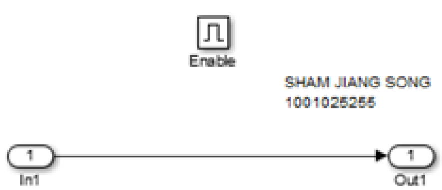

Figure-5. Enabled subsystem.

Figure-6 shows a swing up controller that helps to swing up the pendulum (Md. Akhtaruzzaman, Amir A. Shafie, 2011). Negative angle is absolutes by the Abs block to ensure the comparison is accurate and precious.

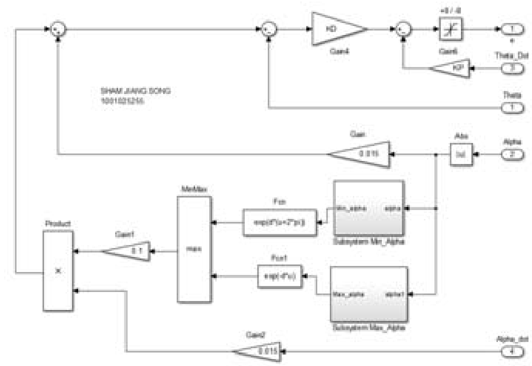

Figure-6. Swing-up controller subsystem.

$e^{d*(u+2*\pi)}$ and e^{-d*u} is a equation to calculate the swing up energy needed by the arm. Value of d, KP and KD is assigned to 1, 0.786 and 9 respectively throughout modelling. Saturation is used to limit input signal to desired upper and lower saturation values.

Figure-7 shows subsystem of min_alpha and Figure-8 shows subsystem max_alpha. Both subsystems are used to choose minimum or maximum inputs generated by IP subsystem. Figure-9 shows an unit delay block which used to hold and delay input by specifying the sample period.

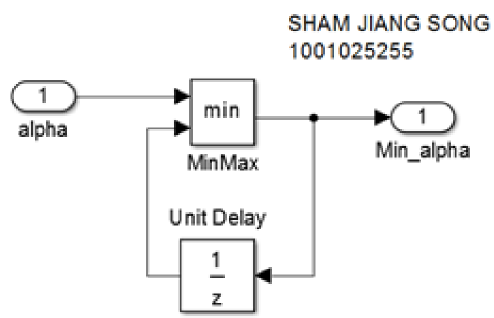

Figure-7. Subsystem min_alpha.

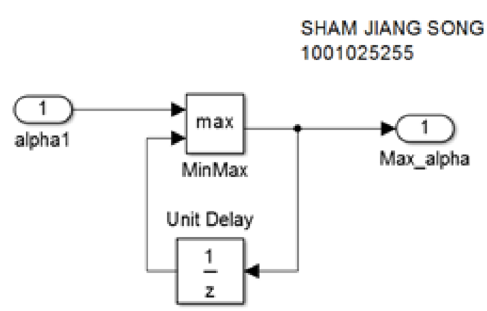

Figure-8. Subsystem max_alpha.

VOL. 10, NO. 20, NOVEMBER 2015 ISSN 1819-6608
ARPN Journal of Engineering and Applied Sciences

www.arpnjournals.com

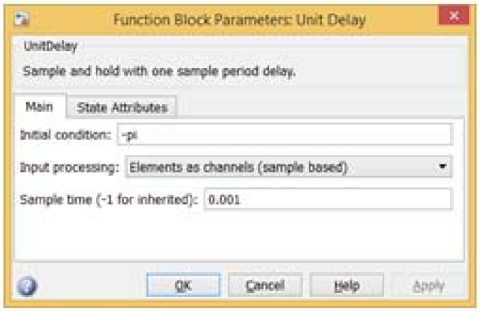

Figure-9. Unit delay block.

Figure-10 shows physical geometry of IP that acts as free body diagram of IP to derive equations of motion by using Langrangian Formula (Quanser Innovate Educate. QNET Experiment #04 Inverted Pendulum Control).

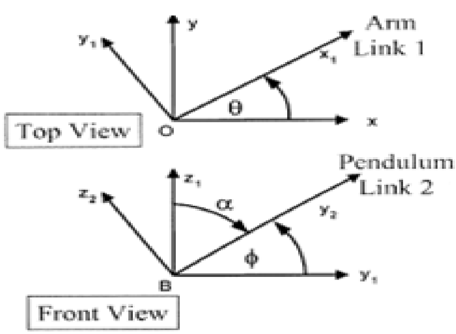

Figure-10. Physical geometry of IP.

Potential Energy,

$$P = \frac{1}{2}J_{eq}\dot{Q}^2 + \frac{1}{2}m\left[\left(r\dot{Q} - L\cos\alpha(\dot{\alpha})\right)^2 + (-L\sin\alpha(\dot{\alpha}))^2\right] + \frac{1}{2}J_B\alpha^2 \quad (1)$$

whereby J_B is $\frac{1}{2}m(2L)^2 = \frac{1}{3}mL^2$ (2)

Substitute equation (2) into equation (1),

$$P = \frac{1}{2}(J_{eq} + mr^2)\dot{Q}^2 + \frac{2}{3}(mL^2\dot{\alpha}^2) - mLr\,(\cos\alpha)(\dot{\theta})(\dot{\alpha}) \quad (3)$$

Kinetic Energy,

$$K = mgl\ \cos\alpha \quad (4)$$

Subtract equation (3) with equation (4),

$$L = \frac{1}{2}(J_{eq} + mr^2)\dot{Q}^2 + \frac{2}{3}(mL^2\dot{\alpha}^2) - mLr\,(\cos\alpha)(\dot{\theta})(\dot{\alpha}) - mgl\ \cos\alpha \quad (5)$$

Two equations according to Langrangian Formulation,

$$\frac{d}{dt}\left(\frac{dL}{d\dot{\theta}}\right) - \frac{dL}{d\theta} = T_1 - B_{eq}\dot{\theta} \quad (6)$$

$$\frac{d}{dt}\left(\frac{dL}{d\dot{\alpha}}\right) - \frac{dL}{d\alpha} = 0 \quad (7)$$

Output torque of driving unit on the load shaft,

$$T_1 = n_g K_g\left(T_m - J_m\ddot{\theta}_m\right) \quad (8)$$

where,

$T_m = n_m K_t I_m$, $\ddot{\theta}_m = K_g\ddot{\theta}$, $I_m = \frac{V_m - K_m K_g\dot{\theta}}{R_m}$

Output torque from equation (8),

$$T_1 = \frac{n_m n_g K_t K_g}{R_m}(V_m) - \frac{n_m n_g K_t K_g^2 K_m}{R_m}\dot{\theta} - n_g K_g^2 J_m\ddot{\theta} \quad (9)$$

Differentiate equation (5) according to equation (6) and (7), the nonlinear model of the system as follows:

$$(J_{eq} + mr^2)\ddot{\theta} - mLr\left((\ddot{\alpha})\cos\alpha - \dot{\alpha}^2\sin\alpha\right) = \frac{n_m n_g K_t K_g}{R_m}(V_m) - \frac{n_m n_g K_t K_g^2 K_m}{R_m}\dot{\theta} - n_g K_g^2 J_m\ddot{\theta} - B_{eq}\dot{\theta} \quad (10)$$

$$\frac{4}{3}(mL^2\ddot{\alpha}) - mLr\left(\ddot{\theta}\cos\alpha\right) - (-mgL(-\sin\alpha)) = 0$$

If $\alpha\ and\ \ddot{\alpha} = 0;\ \sin\alpha = \alpha, \cos\alpha = 1$,
from equation (10),

$$(J_{eq} + mr^2 + n_g K_g^2 J_m)\ddot{\theta} - mLr(\ddot{\alpha}) + \left(B_{eq} + \frac{n_m n_g K_t K_g^2 K_m}{R_m}\right)\dot{\theta} = \frac{n_m n_g K_t K_g}{R_m}(V_m) \quad (11)$$

$$\frac{4}{3}(mL^2)(\ddot{\alpha}) - mLr\ddot{\theta} - mgL\alpha = 0$$

where,

$A = J_{eq} + mr^2 + n_g K_g^2 J_m$ $\quad B = mLr$

$C = \frac{4}{3}(mL^2)$ $\quad D = mgL$

$E = B_{eq} + \frac{n_m n_g K_t K_g^2 K_m}{R_m}$ $\quad F = \frac{n_m n_g K_t K_g}{R_m}$

$G = AC - B^2$

Table-1 Shows the value used throughout the calculation.

Table-1. Parameter table.

Symbol	Description	Value	Unit
g	Gravity acceleration	9.81	m/s^2
B_{eq}	Equivalent viscous damping coefficient	0.001	Nm/(rad/s)
K_g	Motor gear ratio	10	
n_g	Gearbox efficiency	0.9	
K_t	Motor torque constant	0.0183	N*m /A
K_m	Back-emf constant	0.0183	V*s / rad
J_m	Moment of inertia of the rotor of the motor	0.00020181	kg*m^2
R_m	Armature resistance	2.5604	Ω
n_m	Motor efficiency	0.69	
J_{eq}	Equivalent moment of inertia at the load	0.0013	kg* m^2
m	Mass of pendulum	0.022	kg
L	Length to pendulum's center of mass	0.08	m
r	Rotating arm length	0.174	m

Solving equation (11) for two accelerations $\ddot{\theta}$ and $\ddot{\alpha}$,

$$\ddot{\theta} = \frac{1}{G}\begin{bmatrix} -E\dot{\theta} + FV_m & -B \\ D\alpha & C \end{bmatrix}$$

$$\ddot{\theta} = \frac{1}{G}\left(BD\alpha - CE\dot{\theta} + CFV_m\right) \tag{12}$$

$$\ddot{\alpha} = \frac{1}{G}\begin{bmatrix} A & -E\dot{\theta} + FV_m \\ -B & D\alpha \end{bmatrix}$$

$$\ddot{\alpha} = \frac{1}{G}\left(AD\alpha - BE\dot{\theta} + BFV_m\right) \tag{13}$$

Convert into matrix form,

$$\begin{bmatrix} \dot{\theta} \\ \dot{\alpha} \\ \ddot{\theta} \\ \ddot{\alpha} \end{bmatrix} = \begin{bmatrix} 0 & 0 & 1 & 0 \\ 0 & 0 & 0 & 1 \\ 1 & \frac{BD}{G} & -\frac{CE}{G} & 0 \\ 0 & \frac{AD}{G} & -\frac{BE}{G} & 0 \end{bmatrix} \begin{bmatrix} \theta \\ \alpha \\ \dot{\theta} \\ \dot{\alpha} \end{bmatrix} + \begin{bmatrix} 0 \\ 0 \\ \frac{CF}{G} \\ \frac{BF}{G} \end{bmatrix} V_m \tag{14}$$

Equation (14) can be represents as,

$$u = Pu(t) + OV_m \tag{15}$$

Weighting matrices are selected correctly and tested.

R1 = diag ([40,40,0.1,0.5]) R2 = 0.0001

By applying command in MATLAB, the optimal gain is obtained.

K = lqr (P, O, R1, R2)

K = e^3 [-0.6325 1.9925 -0.2126 0.2093]

Ignoring e^3 due to the S.I. units used throughout the project is in millimeter.

$$u = -Kx \tag{16}$$

Equation (16) shows the feedback state equation. Thus, any K values must multiply with negative in MATLAB.

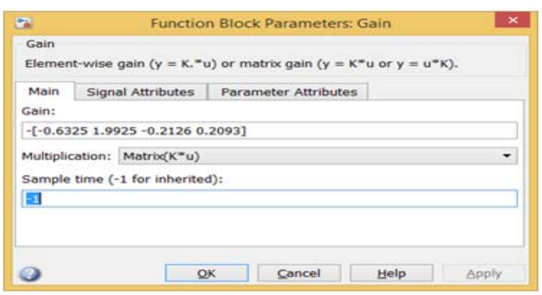

Figure-11. Optimum gain for LQR.

Coding that used in MATLAB Function Block:

```
function y = fcn(u)
if (u > 0)
    y = (3.1459265-u)*180/3.14159265;
else
    y = u *180 / 3.14159265;
end
```

RESULT

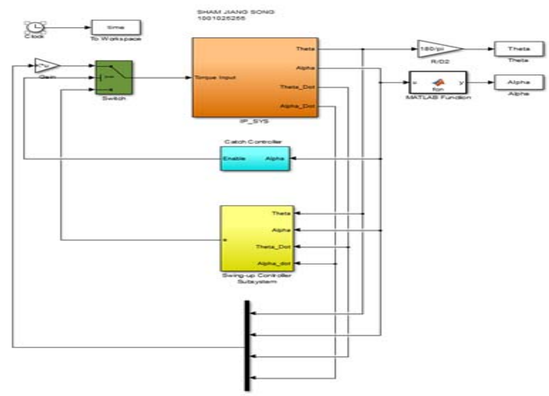

Figure-12. Finalized system.

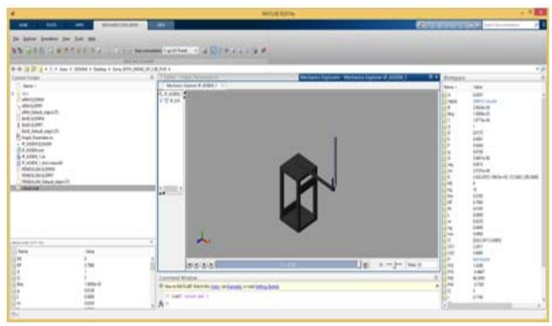

Figure-13. Animation in SimMechanics.

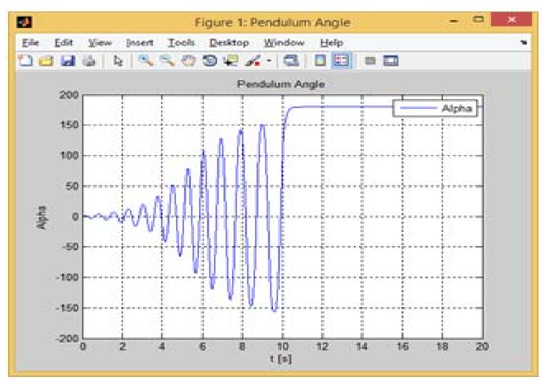

Figure-14. Angle of pendulum from SimMechanics.

ARPN Journal of Engineering and Applied Sciences

www.arpnjournals.com

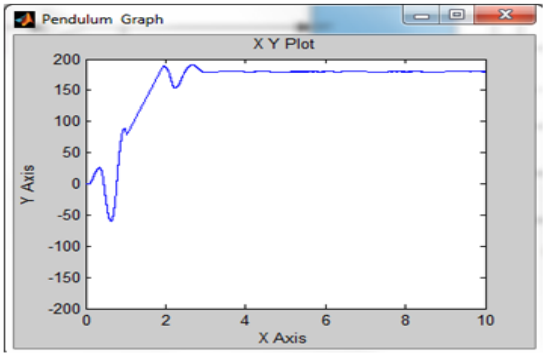

Figure-15. Angle of pendulum from IP experiment.

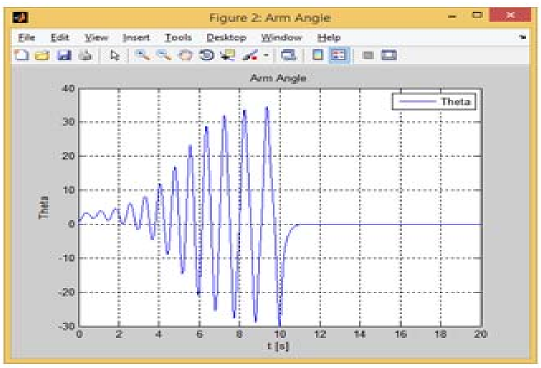

Figure-16. Angle of arm from SimMechanics.

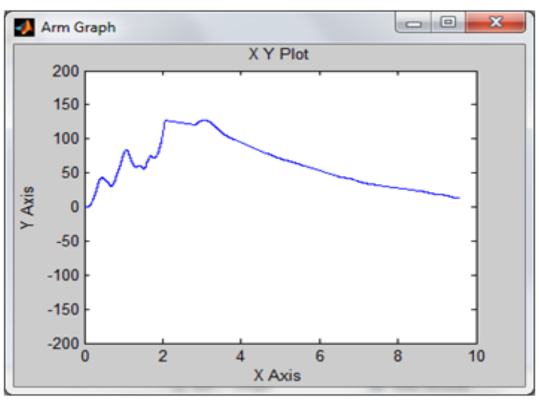

Figure-17. Angle of arm from IP experiment.

CONCLUSIONS

LQR controller was used for both SimMechanics simulation and EMECS simulation. The pendulum stabilized in upright position and the arm reaches desired position. Figure-12 shows final built of IP system in Simulink with block diagrams. Figure-13 shows animation of IP that built in SimMechanics. Figure-14 and Figure-16 shows graph generated by SimMechanics simulation. Figure-15 and Figure-17 shows graph generated by real experiment. Based on graph given, both of them were approximate the same. During calculation of LQR, certain values of parameter were different from datasheet given.

REFERENCES

[1] Astrom K. J. and Furuta K. 1996. Swinging up a Pendulum by Energy Control. Paper presented at IFAC 13th World Congress, San Francisco, Californiapp, pp.1-6.

[2] Darina Hroncova, Miroslav Pastor. 2013. Mechanical System and SimMechanics Simulation. Journal of Mechanical Engineering, Vol. 1, No. 7, pp. 251-255.

[3] Jia-Jun Wang. 2012. Stabilization and tracking control of X-Z inverted pendulum with sliding-mode control. ISA Transactions, Vol. 51, pp. 763-770.

[4] Low K. H., Wang H. and Wang M. Y. 2005. On the development of a real time control system by using xPC target: Solution to robotic system control. Proceedings of the IEEE International Conference on Automation Science and Engineering, Aug. 1-2, Canada, pp. 345-350. DOI: 10.1109/COASE.2005.1506793

[5] Mahadi Hasan, Chanchal Saha, Md. Mostafizur Rahman, Md. Rabiual Isam Sarker, Subrata K. Aditya. 2012. Balancing of an Inverted Pendulum Using PD Controller. Dhaka Univ. J. Sci. Vol. 60, No. 1, pp. 115-120.

[6] K. J. Astrom, K. Furuta 2000. Swinging up a pendulum by energy control. Automatica 36 (2000), pp.287 – 295.

[7] Majid H Koul, Subir K Saha. 2013. Simulation of Haptics Force Law using SimMechanicss and Simulink. 1st International and 16th National Conference on Machines and Mechanisms (iNaCoMM2013).

[8] Mary M. and Marimuthu. 2008. Design of intelligent hybrid controller for swing-up and stabilization of rotary inverted pendulum. ARPN J.Eng. Applied Sci., 3.

[9] Md. Akhtaruzzaman, Amir A. Shafie. 2011. Comparative assessment and result analysis of various control methods, applied on a rotary inverted pendulum, SRV 02 series. Pelagia Research Library, Advances in Applied Science Research, Vol. 2, No. 6, pp. 83-100.

[10] Olfa Boubaker. 2003. The inverted Pendulum: A fundamental Benchmark in Control Theory and Robotics. National Institute of Applied Sciences and Technology.

[11] Quanser Innovate Educate. QNET Experiment #04 Inverted Pendulum Control. Laboratory Manual.

[12] Rogelio Lozano, Isabelle Fantoni, Dan J. Block. (2000). Stabilization of the inverted pendulum around its homoclinic orbit. Systems & Control Letters, 40, pp.197-204.

[13] Sim Mechanics Link User’s Guide. 2015. SimMechanics User’s Guide, pp. 2-2 – 2-5.

[14] Stelian-Emolion Oltean. 2014. Swing-up and stabilization of the rotational inverted pendulum using PD and fuzzy-PD controllers. ScienceDirect Procedia Technology, 12, pp. 57-64.

[15] Viroch Sukontanakarn and Manukid Parnichkun. 2009. Real-Time Optimal Control for Rotary Inverted Pendulum. Mechatronics, School of Engineering and Technology, Asian Institute of Technology, Pathumthani, Thailand.

[16] Xiumin Diao and Dr. Ou Ma. 2006. Rotary Inverted Pendulum. Course Project. New Mexico State University.